Fabrication and Characterization of ALD-grown ZrO_2:Ge Thin Films on Si(1 0 0) using $CpZr(NMe_2)_3$ and $(NMe_2)_2Ge(^{i}pr_2en)$ Precursors with Ozone

Jae-Sun Jung,[†,‡] Dae-Hyun Kim,[‡] Jin-Ho Shin,[‡] Jung-Soo Kang,[§] Joseph P. Thomas,[§] K. T. Leung,[§] and Jun-Gill Kang[†,*]

[†]*Department of Chemistry, Chungnam National University, Daejeon 305-764, Korea.*
**E-mail: jgkang@cnu.ac.kr*
[‡]*Soulbrain Sigma-Aldrich Co., Ltd, Gongju-si 314-240, Korea*
[§]*WATLab and Department of Chemistry, University of Waterloo, Waterloo, Canada*
Received April 1, 2015, Accepted April 25, 2015, Published online July 28, 2015

Keywords: Atomic layer deposition, Ge-doped ZrO_2 thin film, Growth rate

The continuous scaling of complementary metal-oxide semiconductor (CMOS) device dimensions to a few nanometers thick has led to the use of high-dielectric materials. The traditional SiO_2 layer in the application to the nanosized configurations faces a problem, such as the leak currents from electron tunneling through the dielectrics due to its low dielectric constant with $k = 3.9$.[1–3] ZrO_2 is a particularly attractive material[4,5] because of its large dielectric constant ($k > 20$),[1,6] wide band gap (5.8–7.8 eV),[7] and high thermal stability with Si.[8] ZrO_2 has already been used in dynamic random access memory (DRAM); however, incorporation of ZrO_2 into next-generation DRAM devices remains a challenge. Zirconia exists in three polymorphs: monoclinic, tetragonal, and cubic, as well as the amorphous state. The dielectric constants of the monoclinic, tetragonal, and cubic phases are 20, 47, and 37, respectively.[9–11] The monoclinic phase is the most stable, however, and is in equilibrium at room temperature, whereas the tetragonal and cubic phases can be stabilized at temperatures greater than 1400 and 2570 K, respectively. For ultra-thin films, however, the amorphous state is stable up to 750 °C.[12] Recently, doping ZrO_2 with Ge has been shown to increase k,[13–16] which is attributed to favorable formation of the metastable phase. Atomic layer deposition (ALD) has been shown to be an excellent method for deposition of high-quality ultra-thin films for semiconductor device applications;[17] however, few studies have reported the properties of ALD-grown GeO_2, and to date, Ge-doped ZrO_2 thin films have been formed using molecular beam epitaxy at high temperatures. Germanium ALD growth precursors include 1,2-bis[(2,6-diisopropylphenyl)imino] acenaphthene germanium(II), germanium(IV) ethoxide, and tetrakis-(dimethylamino) germanium(IV), which are expensive and limited in supply. We have previously reported an ALD growth process for ZrO_2 and GeO_2 ultra-thin films using cyclopentadienyl-type Zr(IV) and ethylenediamine-type Ge(IV) precursors, respectively. Bis(dimethylamino)(*N*,*N*′-di-isopropyl-ethylenediamine) germanium $[(NMe_2)_2Ge(^{i}pr_2en)]$ with ozone exhibits a distinct temperature-independent plateau in its growth rate, remaining at 0.40 Å/cycle in the range 200–320 °C. Here we describe an ALD growth process for Ge(IV)-doped ZrO_2 ultra-thin films using $CpZr(NMe_2)_3$ and $(NMe_2)_2Ge(^{i}pr_2en)$ with ozone. We investigated the relationships between film thickness, stoichiometry of the precursor mixture, and chemical composition, with the aim of controlling Ge doping and achieving high-quality ZrO_2:Ge thin films on Si(1 0 0).

Three types of ZrO_2:Ge/ZrO_2 multilayer were fabricated on Si(1 0 0) substrates by controlling precursor ratios. Both ALD conditions and the method of injection of the different precursors significantly affected the quality of the resulting films. Table 1 lists the Ge-doped ZrO_2 ALD growth conditions with the $CpZr(NMe_2)_3$ and $[(NMe_2)_2Ge\ (^{i}pr_2en)]$ precursors. Two basic subcycles were designed for separately feeding pure Zr precursor (A) and a mixture of Zr and Ge precursors (B), as shown in Figure 1. Each subcycle corresponded to a pulse sequence, as listed in Table 1; hereafter, pulses for feeding A and B are referred to as cycles A and B, respectively. First, we fabricated the multilayered thin films on Si wafers via a sequence of five consecutive A-cycles, followed by one B-cycle (creating film F1), and the total number of cycles was 198. Two further sets of multilayered thin films were fabricated using the following sequences: three consecutive A-cycles followed by one B-cycle (F2) and one A-cycle, followed by one B-cycle (F3); for all of these, the total number of cycles was 200. The molar ratios of Ge to Zr were 0.09, 0.14, and 0.33 for the F1, F2, and F3 films, respectively.

The thickness of each film was determined using ellipsometry (MG-1000; Nano-View, Seoul, Korea). The film F1 was 213.8 Å thick, and the growth rate was 1.08 Å/cycle. The observed growth rate of the Ge-doped thin films was equal to that of un-doped ZrO_2 thin films grown under identical ALD conditions. As the fraction of B-cycles increased, the thickness of the films decreased (the total number of cycles remained approximately constant at ~200). The F2 film was 208 Å thick and grew at a rate of 1.04 Å/cycle, and the F3 film was 187 Å thick with a growth rate of 0.935 Å/cycle. Given

that the growth rate of a pure GeO_2 thin film grown under identical conditions was 0.4 Å/cycle, these results indicated that Ge concentration increased as the fraction of B-cycles increased.

The surface roughness and film morphology were analyzed using atomic force microscopy (AFM) using a NanoScope V Scanning Probe Microscope (Bruker, Santa Barbara, CA, USA). As shown in Figure 2, the F1 film was relatively smooth, with a root-mean-square (rms) roughness of R_q = 0.59 nm. Increasing Ge content resulted in an increase in the surface roughness: R_q of 0.65 and 1.10 nm for F2 and F3, respectively. The greater surface roughness of the F3 film may be due to the greater mismatch in the growth rates of the Zr and Ge precursors. Even with the F3 film, however, R_q was less than 6% of the film thickness; all films may thus be considered to have a smooth morphology.

The spatially resolved chemical composition of the ZrO_2:Ge/ZrO_2 multilayer structure was characterized using time-of-flight secondary ion mass spectroscopy (TOF-SIMS, ION-TOF GmbH, Münster, Germany). Note that the intensities of carbon and nitrogen were lower than the detection limit. Figure 3 shows depth profiles of Si, Zr, and Ge in the thin films. The Si signal did not exceed the background until 90–120 min, followed by a rapid increase. The region where the intensities of Zr and Ge ions were maintained at a near-constant level can be clearly distinguished prior to the appearance of the Si signal. These results indicated that the Ge dopants were homogeneously distributed throughout the ALD-grown thin film. Figure 4 shows the relative Ge content in the films, which was consistent with the molar ratios of the precursors listed in Table 2. These results indicated that the concentration of the Ge dopant was proportional to the molar ratio of the precursor.

X-ray photoelectron spectroscopy (XPS) data for the three films were obtained following Ar^+ ion sputtering for 10 s using a MultiLab 2000 Thermo Scientific (Waltham, MA, USA) with a monochromatic Al Kα source (1486.6 eV). As shown in Figure 5, peaks corresponding to Zr 3d (170–188 eV) and O 1 s (~530 eV) can be seen, as well as weaker peaks corresponding to Ge 3d (~30 eV), 3p (129–122 eV), and $2p_{3/2}$ (~1220 eV).[18] Characteristic Si 2s (152 eV) and 2p (100 eV) peaks, as well as C 1s (285 eV) and N 1s (402 eV) peaks were not observed, or appeared only as trace features. The highly resolved spectrum of Ge 3p, scanned with a resolution of 0.05 eV, displayed two bands with peaks at 124.1 and

Table 1. ALD growth conditions for a subcycle injection.

Growth conditions	
Evaporation temperature	105 °C
Carrier gas (sccm)	Ar (80)
Reactant gas (sccm)	O_3 (100)
Substrate temperature	300 °C
Working pressure	1 Torr
Pulse sequence (precursor/purge/O_3/purge)	5/10/5/10 s
Number of cycle	198–200

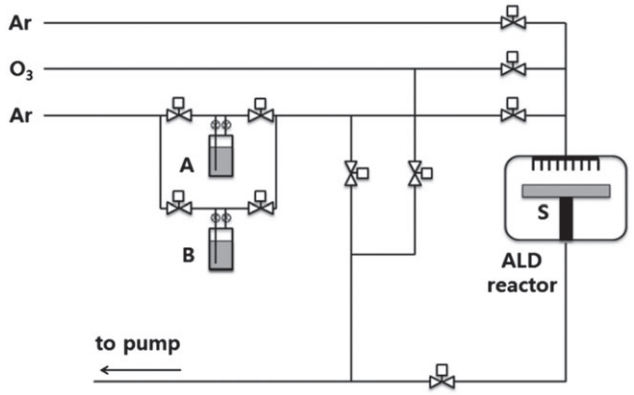

Figure 1. Schematic diagram for injection of two different precursor-compositions—A: a canister containing a pure Zr precursor; B: a canister containing an equivalent mixture of Zr and Ge precusors, S; Si substrate.

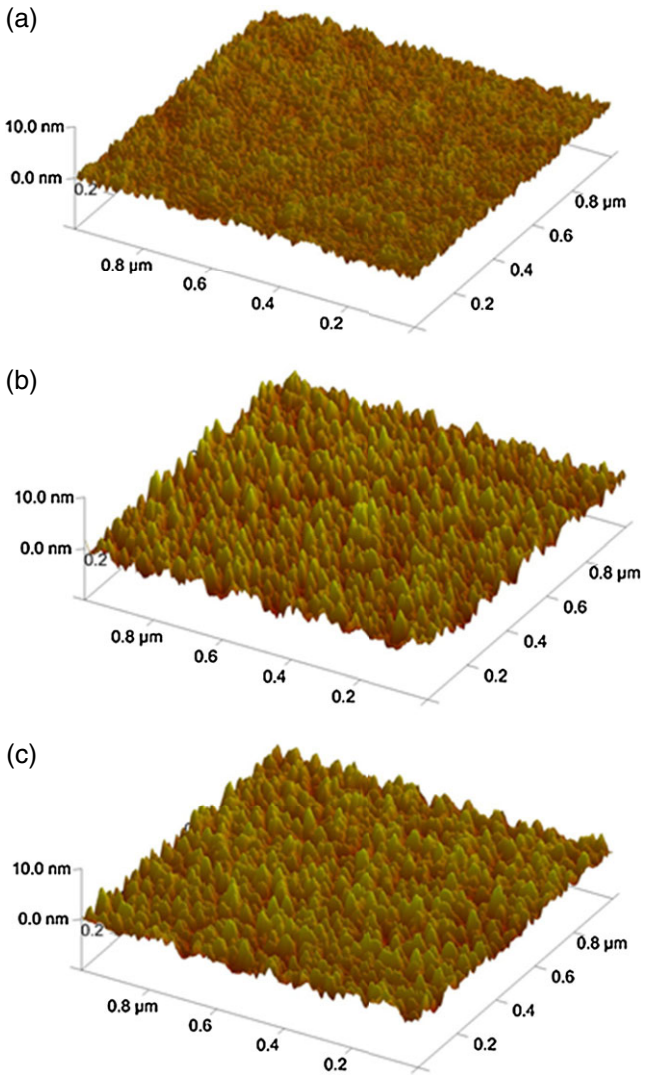

Figure 2. AFM images of Ge-doped ZrO_2 thin film surfaces grown via the ALD process: (a) F1, (b) F2, and (c) F3.

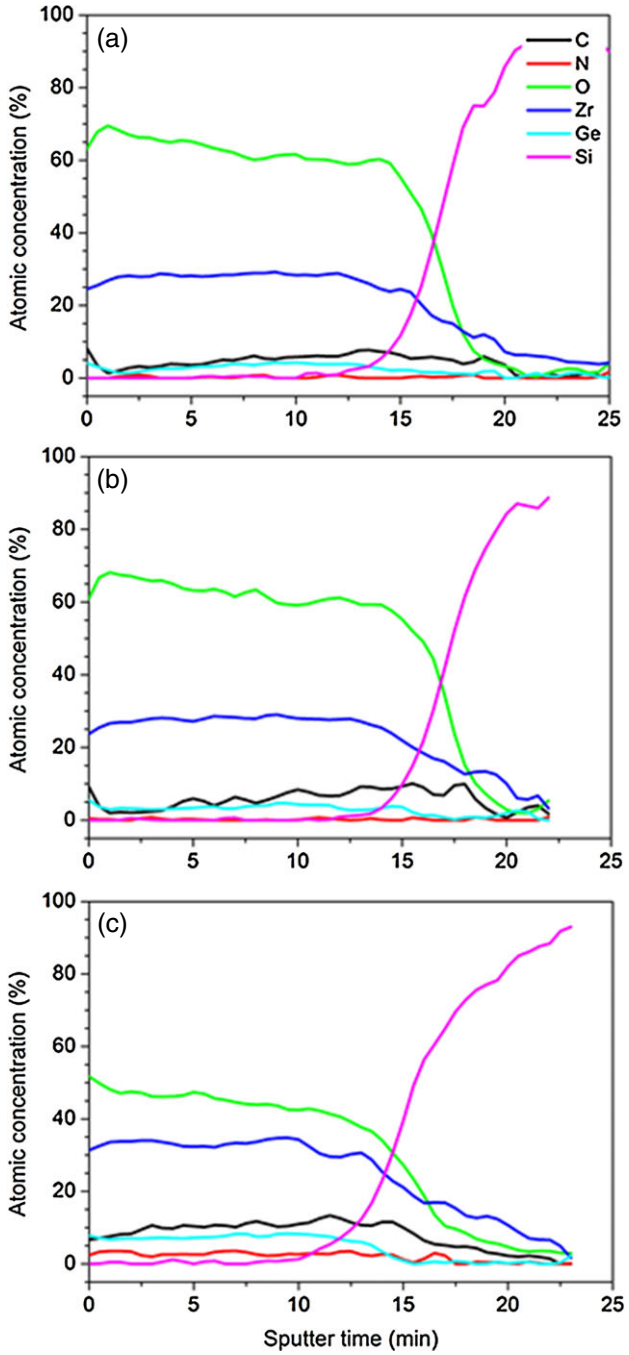

Figure 3. Depth profile performed on (a) F1,(b) F2, and (c) F3.

128.9 eV. The 124.1 eV peak appears as a well-defined line, and can be attributed to Ge $3p_{3/2}$ (Figure 5(b)). We assign the 128.9 eV peak (which appeared with moderate intensity) to the $3p_{1/2}$ line of the ionized Ge dopant, which has not previously been reported. The approximate composition of the Ge atom was determined from the 3p peak area, since the uncertainty in the peak area from $2p_{3/2}$ was too high arisen from its low resolution (1 eV) scanning (Figure 5(c)). As listed in Table 2, the Ge 3p peaks were well-matched with the experimental relative concentration, although the strongest $2p_{3/2}$ peak did not exhibit the expected proportional behavior.

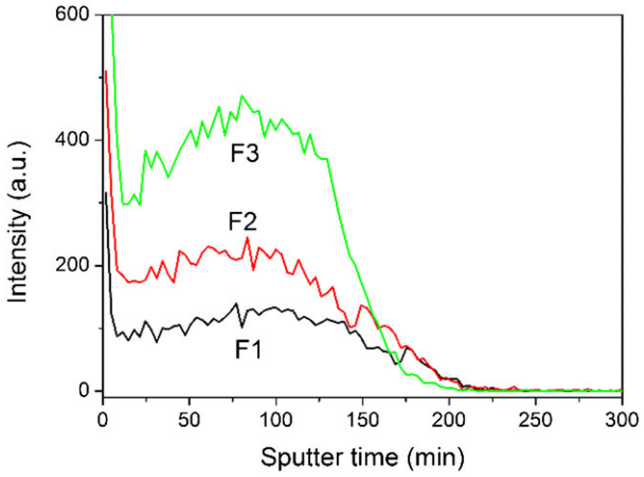

Figure 4. Depth profiles of Ge of the prepared films (the base line was subtracted).

Table 2. Relative Ge concentrations of the F1, F2, and F3 thin films.

Film	Injection (mole ratio)	TOF-SIMS	XPS (3p)
F1	1 (0.09)	1	1
F2	1.6 (0.14)	1.7	1.6
F3	3.7 (0.33)	3.3	3.4

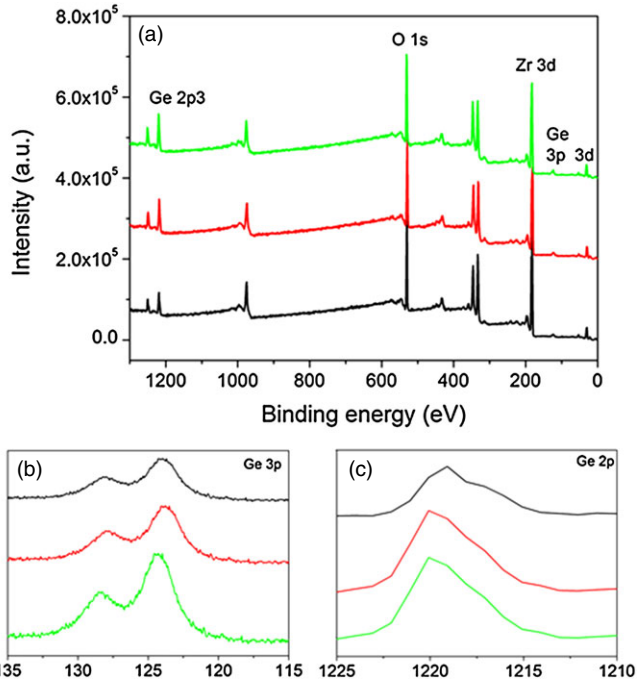

Figure 5. XPS spectra of the F1 (black), F2 (red), and F3 (green) films treated by Ar^+ ion sputtering (a) for 10s, and bands of (b) Ge 3p and (c) Ge 2p.

In conclusion, we have demonstrated high-quality Ge-doped ZrO_2 thin films via ALD using the precursors $CpZr(NMe_2)_3$ and $(NMe_2)_2Ge(^ipr_2en)$. A dual-subcycle system was used to separately feed the Zr precursor and a mixture

of the Zr and Ge precursors, which was crucial in growing films without forming precipitates. The growth rate and dopant concentration were characterized as a function of the number of subcycles of the mixed precursors. The growth rates with Ge mole fractions of 0.09, 0.14, and 0.33 were 1.08, 1.04, and 0.935 Å/cycle, respectively. These thin films had a smooth surface morphology, and the carbon and nitrogen impurity concentrations were smaller than the detection limit of the TOF-SIMS system.

Experimental

Synthesis. To synthesize $CpZr(NMe_2)_3$, 4.21 mol of *n*-BuLi dissolved in hexane was added to a 10-L flask containing 3.3 L of toluene, then cooled to a temperature in the range −20 to −15 °C. $HNMe_2$ (5.46 mol) was slowly bubbled and white precipitate of $LiNMe_2$ formed immediately. The mixture was warmed to 60 °C for 5 h. Following removal of excess $HNMe_2$, the mixture was cooled to room temperature, and $ZrCl_4$ (1.0 mol) was slowly added to the stirred solution. The reaction mixture was refluxed at 80 °C for 4 h to form the crude $Zr(NMe_2)_4$. The addition of cyclopentadiene monomer to the crude $Zr(NMe_2)_4$ cooled at −15 to −10 °C produced $CpZr(NMe_2)_3$. The solid was removed by filtration and all volatile species were removed by evaporation. The product (61% yield) was obtained by fractional vacuum distillation. ^{1}H NMR (C_6D_6): δ 6.06 (s, 4H), 2.92 (s, 18H). The $(NMe_2)_2Ge(^ipr_2en)$ was synthesized in a 5-L three-neck flask filled with 2.5 L of toluene, and 0.28 mol of $GeCl_4$ was added and then cooled to a temperature in the range −20 °C to −15 °C. Following the gradual addition of 0.25 mol of *N*,*N*′-di(*iso*propyl)ethylenediamine and 0.84 mol of $N(C_2H_5)_3$, the mixture was warmed to room temperature and stirred for 5 h to form $(^ipr_2en)GeCl_2$. The mixture was then cooled to between −20 and −10 °C, 0.88 mol of $Li(NMe_2)$ was added, and the mixture was refluxed at 110 °C for 12 h to form the crude $(NMe_2)_2Ge(^ipr_2en)$. The solid was removed by filtration and all volatile species were removed by evaporation. The product (47.5% yield) was obtained by fractional vacuum distillation.

Atomic Layer Deposition. Ge-doped ZrO_2 films were deposited on Si(1 0 0) substrates using a showerhead-type hot-wall ALD reactor (ASM Genitech, Inc., Seungnam, Korea). The working pressure during deposition was 1 Torr; Table 1 lists a summary of the ALD growth conditions. Argon (>99.999%) and ozone (99.999%) were used as carrier and reactant gases, respectively. The p-type Si substrates (LG Siltron Inc., 2 × 2 cm) were washed using a mixture of H_2SO_4 and H_2O (at a volume ratio of 3:1) for 10 min, then rinsed in deionized water. The substrate was then washed in HF solution (1 vol%) for 1 min and then rinsed in deionized water before loading into the reactor.

References

1. G. D. Wilk, R. M. Wallace, J. M. Anthony, *J. Appl. Phys.* **2001**, *89*, 5243.
2. J. L. Padilla, F. Gámiz, A. Godoy, *Appl. Phys. Lett.* **2013**, *103*, 112105.
3. D. Panda, T.-Y. Tseng, *Thin Solid Films* **2013**, *531*, 1.
4. W. Zhang, Y. Cui, Z. G. Hu, W. L. Yu, J. Sun, N. Xu, Z. F. Ying, J. D. Wu, *Thin Solid Films* **2012**, *520*, 6361.
5. K. Kato, T. Saito, S. Shibayama, M. Sakashita, W. Takeuchi, N. Taoka, O. Nakatsuka, S. Zaima, *Thin Solid Films* **2014**, *557*, 192.
6. S. H. Jeong, I. S. Bae, Y. S. Shin, S.-B. Lee, H.-T. Kwak, J.-H. Boo, *Thin Solid Films* **2005**, *475*, 354.
7. J. Robertson, *J. Vac. Sci. Technol. B* **1785**, *2000*, 18.
8. T. S. Jeon, J. M. White, D. L. Kwong, *Appl. Phys. Lett.* **2001**, *78*, 368.
9. X. Zhao, D. Vanderbilt, *Phys. Rev. B* **2002**, *65*, 075105.
10. S. K. Kim, C. D. Hwang, *Electrochem. Solid-State Lett.* **2008**, *11*, G9.
11. S. Sayan, N. V. Nguyen, J. Ehrstein, T. Emge, E. Garfunkel, M. Croft, X. Zhao, D. Vanderbilt, I. Levin, E. P. Gusev, H. Kim, P. J. McIntyre, *Appl. Phys. Lett.* **2005**, *86*, 152902.
12. J. P. Chang, Y.-S. Lin, *Appl. Phys. Lett.* **2001**, *79*, 3666.
13. D. Tsoutsou, G. Apostolopoulos, S. F. Galata, P. Tsipas, A. Sotiropoulos, G. Mavrou, Y. Panayiotatos, A. Dimoulas, A. Lagoyannis, A. G. Karydas, V. Kantarelou, S. Harissopoulos, *J. Appl. Phys.* **2009**, *106*, 024107.
14. D. Tsoutsou, G. Apostolopoulos, S. F. Galata, P. Tsipas, A. Sotiropoulos, G. Mavrou, Y. Panayiotatos, *Microelectron. Eng.* **2009**, *86*, 1626.
15. Y.-H. Wu, C.-C. Lin, L.-L. Chen, Y.-C. Hu, J. R. Wu, M.-L. Wu, *Appl. Phys. Lett.* **2011**, *98*, 013506.
16. F. Boscherini, F. D'Acapito, S. F. Galata, D. Tsoutsou, A. Dimoulas, *Appl. Phys. Lett.* **2011**, *99*, 121909.
17. A. M. George, *Chem. Rev.* **2010**, *110*, 111.
18. A. V. Naumkin, A. Kraut-Vass, S. W. Gaarenstroom, C. J. Powell, *NIST X-ray Photoelectron Spectroscopy Data V. 4.1, the Measurement Services Division of the National Institute of Standards and Technology*, **2012**.

